8. De Souza B, Brunetti A, Fulham MJ, et al. Pituitary microadenomas: a PET study. Radiology 1990;177:39–44.
9. Kaye TB, Crapo L. The Cushing's syndrome: an update on diagnostic tests. Ann Intern Med 1990;112:433–444.
10. Gold EM. The Cushing syndromes: changing views of diagnosis and treatment. Ann Intern Med 1979;90:829–844.
11. Brooks RA, Friauf WS, Sank VJ, Cascio HE, Leighton SB, Di Chiro G. Initial evaluation of a high resolution positron emission tomograph. In: Greitz T, Ingvar DH, Widen L, eds. The metabolism of the human brain studied with positron emission tomography. New York: Raven Press; 1985:351–361.
12. Sokoloff L, Reivich M, Kennedy C, et al. The ^{14}C-deoxyglucose method for the measurement of local cerebral glucose utilization: theory procedure and normal values in the conscious and anesthetized albino rat. J Neurochem 1977;28:897–916.
13. Brooks RA. Alternative formula for glucose utilization using labeled deoxyglucose. J Nucl Med 1982;23:538–539.
14. Phelps ME, Huang SC, Hoffman EJ, Selin C, Sokoloff L, Kuhl DE. Tomographic measurement of local cerebral glucose metabolic rate in humans with [^{18}F]2-fluoro-2-deoxy-d-glucose: validation of method. Ann Neurol 1979;6:371–388.
15. Reivich M, Alavi A, Wolf AP. Glucose metabolic rate kinetic model parameter determination in man: the lumped constants and rate constants for [^{18}F]fluorodeoxy-glucose and [^{11}C]deoxyglucose. J Cereb Blood Flow Metab 1985;5:179–192.
16. Fulham MJ, Brunetti A, Aloj L, Raman R, Dwyer AJ, Di Chiro G. Decreased brain glucose metabolism in patients with brain tumors: an effect of corticosteroids. J Neurosurg 1995;83:657–664.
17. Cohen SM. Cushing's syndrome: a psychiatric study of 29 patients. Br J Psychol 1980;136:120–124.
18. Jeffcoate WJ, Silverstone JT, Edwards CRW, Besser GM. Psychiatric manifestations of Cushing's syndrome: response to lowering of plasma cortisol. QJ Med 1979;48:465–472.
19. Starkman MN, Scheingart SE. Neuropsychiatric manifestations of patients with Cushing's syndrome: relationship to cortisol and adrenocorticotropic hormone levels. Arch Intern Med 1981;141:215–219.
20. Hatazawa J, Brooks RA, Di Chiro G, Bacharach SL. Glucose utilization rate versus brain size in humans. Neurology 1987;37:583–588.
21. Evans RM, Arriza JL. A molecular framework for the actions of glucocorticoid hormones in the nervous system. Neuron 1989;2:1105–1111.
22. Horner HC, Packan DR, Sapolsky RM. Glucocorticoids inhibit glucose transport in cultured hippocampal neurons and glia. Neuroendocrinology 1990;52:57–64.
23. Packan DR, Sapolsky RM. Glucocorticoid endangerment of the hippocampus: tissue steroid and receptor specificity. Neuroendocrinology 1990;51:613–618.
24. Sapolsky RM, Uno H, Rebert CR, Finch CE. Hippocampal damage associated with prolonged glucocorticoid exposure in primates. J Neurosci 1990;10:2897–2902.
25. McEwen BS, de Kloet ER, Rostene W. Adrenal steroid receptors and actions in the nervous system. Phys Rev 1986;66:1121–1188.
26. Ahima RS, Harlan RE. Charting of Type II glucocorticoid receptor-like immunoreactivity in the rat central nervous system. Neuroscience 1990;39:579–604.
27. Olgemoller B, Schon J, Wieland O. Endothelial plasma membrane is a glucocorticoid regulated barrier for the uptake of glucose in to the cell. Mol Cell Endocrinol 1985;43:165.
28. Horner HC, Munck A, Lienhard GE. Dexamethasone causes translocation of glucose transporters from the plasma membrane to an intracellular site in human fibroblasts. J Biol Chem 1987;262:17696–17702.
29. Sokoloff L. Cerebral circulation, energy metabolism and protein synthesis: general characteristics and principles of measurement. In: Phelps ME, Mazziotta JC, Schelbert HR, eds. Positron emission tomography and autoradiography: principles and applications in the brain and heart. New York: Raven Press; 1986:1–71.
30. Momose KJ, Kjellber RN, Kliman B. High incidence of cortical atrophy of the cerebral and cerebellar hemispheres in Cushing's disease. Radiology 1971;99:341–348.
31. Bentson J, Reza M, Winter J, Wilson G. Steroids and apparent cerebral atrophy on computed tomography scans. J Comput Assist Tomogr 1978;2:16–23.
32. Okuno T, Ito M, Konishi Y, Yoshioka M, Nakano Y. Cerebral atrophy following ACTH therapy. J Comput Assist Tomogr 1980;4:20–23.
33. Baxter LR, Schwartz JM, Phelps ME, et al. Reduction of prefrontal cortex glucose metabolism common to three types of depression. Arch Gen Psychiatry 1989;46:243–250.
34. Silfverskiold P, Risberg J. Regional cerebral blood flow in depression and mania. Arch Gen Psychiatry 1989;46:253–259.
35. Uytenhoef P, Portelange P, Jacquy J, et al. Regional cerebral blood flow and lateralized hemispheric dysfunction in depression. Br J Psychiatry 1987;143:128–132.

Technetium-99m-ECD SPECT Fails to Show Focal Hyperemia of Acute Herpes Encephalitis

Franz Fazekas, Gudrun Roob, Franz Payer, Peter Kapeller, Siegrid Strasser-Fuchs and Reingard M. Aigner
Department of Neurology, MR Institute, Graz; and Department of Radiology, Section of Nuclear Medicine, Karl-Franzens University, Graz, Austria

This is a case of herpes simplex encephalitis (HSE) examined with ^{99m}Tc-ethyl cysteinate dimer (ECD) and ^{99m}Tc-hexamethyl propyleneamine oxime (HMPAO) SPECT. Static images obtained with ^{99m}Tc-ECD showed a reduced tracer uptake of the temporal lobe but focal hyperactivity using ^{99m}Tc-HMPAO. Dynamic images indicated regional increase of cerebral blood perfusion with both tracers. Technetium-99m-ECD had rapid washout from the inflammed tissue, while ^{99m}Tc-HMPAO had avid uptake. Hypofixation of ^{99m}Tc-ECD leads to failure to detect the characteristic finding of temporal lobe hyperemia in acute HSE.

Key Words: herpes simplex encephalitis; technetium-99m-ethyl cysteinate dimer; technetium-99m-hexamethyl propyleneamine oxime; tracer uptake; SPECT

J Nucl Med 1998; 39:790–792

Technetium-99m-ethyl cysteinate dimer (^{99m}Tc-ECD) has been proposed as a safe and effective marker of regional cerebral perfusion. In normal controls and patients with chronic neurologic disorders, the distribution of ECD was shown to be linearly related to regional cerebral blood flow

as measured by SPECT with ^{133}Xe with only mild underestimation of flow at the high end of the normal range (1). In comparison to ^{99m}Tc-hexamethyl propyleneamine oxime (^{99m}Tc-HMPAO), the distribution of both tracers appeared initially to be similar with the advantage that ^{99m}Tc-ECD had greater radiochemical stability and more rapid washout from extracerebral tissues (2,3). Subsequently, it is reported that ^{99m}Tc-ECD does not show reperfusion hyperemia in the subacute phase of a stroke (4,5). We present a case in which ^{99m}Tc-ECD fails to show hyperemia associated with focal cerebral inflammation. Focal hyperactivity of the temporal lobe has been considered a hallmark finding of acute herpes simplex encephalitis (HSE) on static brain SPECT (6–9) using ^{99m}Tc-HMPAO.

CASE REPORT

A 73-yr-old woman with a headache and subfebrile temperature had become confused over the course of a few days. Neurologic findings consisted of short episodes of aphasia and a mild right hemiparesis. There was a past history of two ischemic strokes, and CT of the head showed leukoaraiosis with old lacunar lesions of the basal ganglia bilaterally. A diagnosis of cerebrovascular disease aggravated by some infectious process was considered. Further deterioration with psychotic symptoms and somnolence prompted
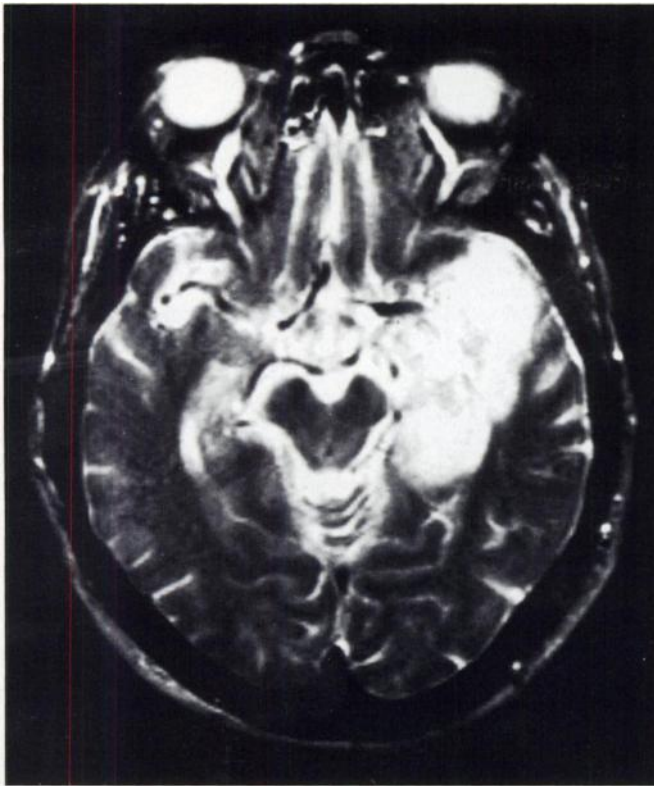
FIGURE 1. Spin-echo T2-weighted brain MRI (TR 2500 msec/TE 90 msec) shows a large area of hyperintensity with a mild mass effect in mediotemporal lobe.

FIGURE 3. Time course of tracer activities in the inflamed temporal lobe region compared to the corresponding contralateral side.

a lumbar puncture (97 lymphoplasmoid cells; total protein 87 mg/dl) and MRI of the brain that showed a mass lesion in the left mediotemporal lobe (Fig. 1). Brain SPECT images were obtained to evaluate a diagnosis of herpes simplex encephalitis (HSE).

Studies were performed with the Tomomatic 564 (Medimatic, Copenhagen, Denmark) consisting of an array of four rotating banks each containing 16 detectors. Dynamic data acquisition at intervals of 30 sec after bolus injection was performed with a low-resolution collimator yielding five contiguous slices. Static images were obtained as two subsequent sets of three interleaved axial slices with a collimation yielding an in-plane resolution of 7.3 mm and an average slice thickness of 9.76 mm at FWHM.

Static SPECT with ^{99m}Tc-ECD showed a focal area of hypoactivity corresponding to the temporal lobe lesion shown on MRI (Fig. 2A). Dynamic data collection, however, showed an increased
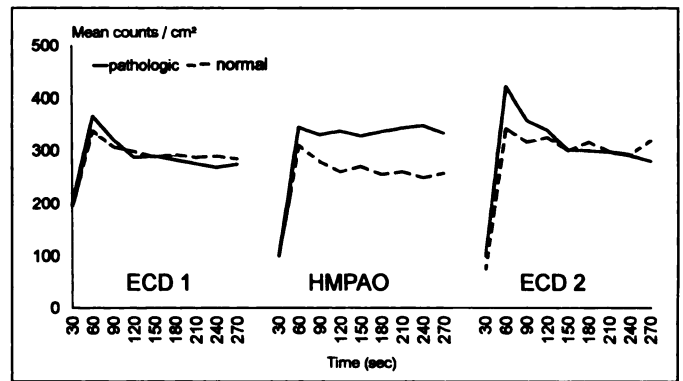
tracer concentration in the left temporal lobe region immediately after injection that suggested hyperperfusion. Another SPECT study with [99m]Tc- HMPAO 1 day later confirmed increased tracer delivery to the left temporal lobe and showed a corresponding area of marked hyperactivity on static images (Fig. 2B). Technetium-99m-ECD SPECT was repeated 2 days later with similar findings to the initial study. Figure 3 compares the course of tracer uptake between the ^{99m}Tc-ECD and ^{99m}Tc-HMPAO studies in the inflamed temporal lobe and the corresponding region of interest on the contralateral side. Hyperactivity of the involved side is clearly noted in all three studies 1 min after tracer injection. Thereafter, both ^{99m}Tc-ECD studies show rapid decrease in tracer activity in the inflamed region with a reduction below the counting rates of the normal tissue. In contrast, ^{99m}Tc-HMPAO is retained in the involved area without washout.

After ^{99m}Tc-HMPAO SPECT, the patient was put on acyclovir. Polymerase chain-reaction studies confirmed a herpes simplex virus infection. MRI signal abnormalities in the temporal lobe regressed and the patient made a good recovery except for residual cognitive deficits.

DISCUSSION

SPECT has been advocated as a sensitive and rather specific tool for the early diagnosis of HSE (6–9). Using ^{99m}Tc-HMPAO or ^{123}I-iodoamphetamine, increased tracer uptake was noted in the acute phase of the disease even before any morphologic abnormalities had become visible or were matching the lesions seen on CT or MRI. Consistent with neuropathologic observations, hyperactivity typically involves the mesiotemporal region and may spread to the adjacent basal ganglia. Based on these data, the regional hypoactivity seen in our
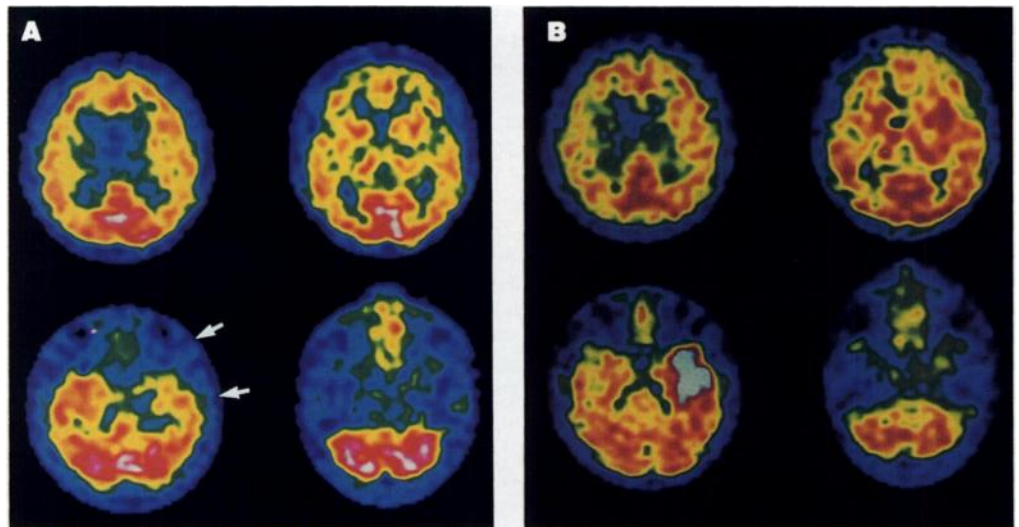

FIGURE 2. (A) Static ^{99m}Tc-ECD SPECT shows focal hypoactivity corresponding to MRI lesion. (B) The same region appears markedly hyperactive on ^{99m}Tc-HMPAO SPECT image 1 day later.

patient on ^{99m}Tc-ECD SPECT was thought to exclude HSE. The expected hyperactivity of the temporal lobe was seen when the patient was reevaluated with ^{99m}Tc-HMPAO.

Technetium-99m-ECD and ^{99m}Tc-HMPAO are both lipophilic agents that penetrate the normal blood-brain barrier. Both are retained by conversion of the lipophilic molecule into hydrophilic compounds. Technetium-99m-ECD is hydrolized to polar metabolites by deesterification (10). The decrease of ^{99m}Tc-ECD activity on dynamic SPECT of our patient indicates the absence or reduction of this enzymatic process in the inflammatory lesion of HSE. The resulting lack of retention causes the pathologic area to appear hypoactive despite the initial presence of hyperperfusion.

Similar observations have been made in the subacute phase of an ischemic stroke where ^{99m}Tc-ECD was noted to miss reflow hyperemia (4,5). In such a setting, this need not constitute a significant disadvantage as the failure to achieve the enzymatic transformation of ^{99m}Tc-ECD may be a better indicator of the extent of tissue damage and prognosis than the visualization of hyperemia (5,11). The inability to detect hyperemia with ^{99m}Tc-ECD in the presence of cellular dysfunction must be viewed differently when considering HSE. Routinely performed dynamic data collection can reduce this problem, but these images have limited resolution and may not be available.

CONCLUSION

Dynamic acquisition following the administration of ^{99m}Tc-HMPAO, ^{123}I-IMP or ^{99m}Tc-ECD demonstrates regional hyperemia of the temporal lobe in HSE. Technetium-99m-ECD, how-ever, washes out. Consequently, hyperemia characteristic of HSE is not detected in clinical SPECT images acquired 2 min later.

REFERENCES

1. Devous MD, Sr, Payne JK, Lowe JL, Leroy RF. Comparison of technetium-99m-ECD to Xenon-133 SPECT in normal controls and in patients with mild to moderate regional cerebral blood flow abnormalities. *J Nucl Med* 1993;34:754-761.
2. Léveillé J, Demonceau G, Walovitch RC. Intrasubject comparison between technetium-99m-ECD and technetium-99m-HMPAO in healthy human subjects. *J Nucl Med* 1992;33:480-484.
3. Pupi A, Castagnoli A, De Cristofaro MTR, Bacciottini L, Petti AR. Quantitative comparison between ^{99m}Tc-HMPAO and ^{99m}Tc-ECD: measurement of arterial input and brain retention. *Eur J Nucl Med* 1994;21:24-130.
4. Lassen NA, Sperling B. Technetium-99m-bicisate reliably images CBF in chronic brain diseases but fails to show reflow hyperemia in subacute stroke: report of a multicenter trial of 105 cases comparing ^{133}Xe and ^{99m}Tc-bicisate (ECD, Neurolite) measured by SPECT on same day. *J Cereb Blood Flow Metab* 1994;14(suppl 1):S44-S48.
5. Tsuchida T, Nishizawa S, Yonekura Y, et al. SPECT images of technetium-99m-ethyl cysteinate dimer in cerebrovascular diseases: comparison with other cerebral perfusion tracers and PET. *J Nucl Med* 1994;35:27-31.
6. Launes J, Nikkinen P, Lindroth L, Brownell A, Liewebdahl K, Iivanainen M. Diagnosis of acute herpes simplex encephalitis by brain perfusion single photon emission computed tomography. *Lancet* 1988;2:1188-1191.
7. Schmidbauer M, Podreka I, Wimberger D, et al. SPECT and MR imaging in herpes simplex encephalitis. *J Comput Assist Tomogr* 1991;15:811-815.
8. McEwan JR, Park CH, Kim SM, et al. Technetium-99m exametazime brain SPECT and magnetic resonance images in the diagnosis of herpes simplex encephalitis. *Clin Nucl Med* 1994;19:66-68.
9. Kao CH, Wang SJ, Mak SC, Shian WJ, Chi CS. Viral encephalitis in children: detection with technetium-99m HMPAO brain single-photon emission CT and its value in prediction of outcome. *Am J Neuroradiol* 1994;15:1369-1373.
10. Walovitch RC, Hill TC, Garrity ST, et al. Characterization of technetium-99m-L,L-ECD for brain perfusion imaging. Part 1: pharmacology of technetium-99m-ECD in nonhuman primates. *J Nucl Med* 1989;30:1892-1901.
11. Brass LM, Walovitch RC, Joseph JL, et al. The role of single-photon emission computed tomography brain imaging with ^{99m}Tc-bicisate in the localization and definition of mechanism of ischemic stroke. *J Cereb Blood Flow Metab* 1994;14(suppl 1):S91-S98.

Reproducibility of the Distribution of Carbon-11-SCH 23390, a Dopamine D₁ Receptor Tracer, in Normal Subjects

Grace L.-Y. Chan, James E. Holden, A. Jon Stoessl, Doris J. Doudet, Yue Wang, Teresa Dobko, K. Scott Morrison, Joe M. Huser, Carolyn English, Barbara Legg, Michael Schulzer, Donald B. Calne and Thomas J. Ruth

TRIUMF and Neurodegenerative Disorders Centre, University of British Columbia, Vancouver, British Columbia, Canada; and Department of Medical Physics, University of Wisconsin, Madison, Wisconsin

The reproducibility of [^{11}C]SCH 23390 in PET was studied in 10 normal human subjects. **Methods:** The scan-to-scan variation of several measures used in PET data analysis, including the radioactivity ratio, plasma-input Logan total distribution volume (DV), plasma-input Logan DV ratio (DVR) and tissue-input Logan B_{max}/K_d values, was determined. **Results:** There were significant correlations among the radioactivity ratio, plasma-input DVR and tissue-input B_{max}/K_d. With the cerebellum as the reference region, these three measures also had high reliability (86%-95%), high between-subject s.d. (7.7%-11.3%) and small within-subject s.d. (2.3%-3.6%), indicating that they are comparable and useful measures for the assessment of dopamine D₁ receptor binding. **Conclusion:** The radioactivity ratio and the tissue-input B_{max}/K_d may be preferred methods for the evaluation of dopamine D₁ receptor binding because these two methods do not require arterial blood sampling and metabolite analysis. Our results show that cerebellum is a reliable reference region for SCH 23390. When the Logan plasma-input function method is used in data analysis for SCH 23390, DVRs rather than total DV values should be used because of the poor reliability of the DV values and their lack of correlation with other measures. Carbon-11-SCH 23390 is thus a reliable and reproducible ligand for the study of dopamine D₁ receptor binding by PET.

Key Words: carbon-11-SCH 23390; PET imaging

J Nucl Med 1998; 39:792-797

The tracer [^{11}C]SCH 23390 is widely used as a ligand to study dopamine D₁ receptor function using PET (1-4). The binding of SCH 23390 to dopamine D₁ receptors, as determined by PET, can be assessed by several methods. The simplest method uses the ratio of activity in regions of high specific binding (such as striatum) to those of nonspecific binding (such as cerebellum). Another method measures the distribution volume (DV) of the ligand in specific and nonspecific regions of